Mechanics of Time-Dependent Materials (2022) 28:485–499
https://doi.org/10.1007/s11043-022-09584-7

Modeling of a homogeneous isotropic half space in the context of multi-phase lag coupled thermoelasticity

Abhijit Lahiri[1] · Sumit Sovan Sardar[2] · Debkumar Ghosh[3]

Received: 1 August 2022 / Accepted: 4 December 2022 / Published online: 21 December 2022

Abstract
A two-dimensional multi-phase lag model in the context of generalized thermoelasticity is established for an isotropic half-space medium. A vector-matrix differential equation is obtained from the governing equations using normal mode analysis. The eigenvalue approach is applied to obtain the solutions. The temperature-dependent displacements, stresses, strains are calculated numerically and represented graphically to show the accuracy of the solution under mechanical and thermal loads.

Keywords Eigenvalue approach · Generalized thermoelasticity · Normal mode analysis and vector-matrix differential equation

1 Introduction

The modified coupled stress-strain theory has become popular in Nano-systems to study strain, displacement, vibration, buckling, bending, etc., in the engineering structures like beams, plates and shells. The modified theory of coupled stress has been introduced by Yang et al. (2002). The theory of generalized thermoelasticity was introduced to remove the finiteness of the heat equation in the conventional classical thermoelasticity (CTE) theory. The generalized thermoelasticity theory has become acceptable to the different engineering fields as well as to the researcher as it is capable of avoiding the finiteness of heat propagation.

✉ D. Ghosh
debkumarghosh2020@gmail.com

A. Lahiri
lahiriabhijit2000@yahoo.com

S.S. Sardar
sssardarpumath@gmail.com

[1] Department of Mathematics, Jadavpur University , Jadavpur, Kolkata, 700032, West Bengal, India

[2] Department of Mathematics, R.K.M. Resedential College (Autonomous), Narendrapur, Kolkata, 700103, West Bengal, India

[3] Department of Mathematics, Eminent College of Management and Technology, Barasat, North 24 Parganas, 700126, West Bengal, India

In the history of generalized thermoelasticity, Lord and Shulman (1967) introduced a one-relaxation time parameter in the conventional heat conduction equation to modify classical Fourier law (CFL), which is also known as the first generalization theory of thermoelasticity. In the second generalization theory, Green and Lindsay (1972) proposed temperature rate dependent theory (TRDTE) by introducing two relaxation time parameters in the coupled theory of thermoelasticity. In the third generalization, Hetnarski and Ignaczak (1996) proposed the non-linear model introducing the concept of coupled thermoelasticity with low temperature. Green and Naghdi (1991, 1992, 1993) proposed three thermoelastic models known as Green-Naghdi type-I, type-II and type-III, respectively. Type-I is considered similar to the classical theory of thermoelasticity. Type-II model provides the idea of non-dissipation of energy associated with zero production rate of entropy. Type-III Green-Naghdi model is associated with type-I and type-II together with the study of energy dissipation and damped thermoelastic waves. Later on, Tzou (1995, 1999) and Chandrasekhariah (1998) discussed the Dual Phase Lag (DPL) model to inspect the lagging behavior in the thermoelastic medium. Again, Roy Choudhuri (2007) discussed the concept of the Three Phase Lag Model [TPL], introducing three-time parameters in the conventional heat conduction equation. Ghosh et al. (2019), Ghosh and Lahiri (2020), Quintanilla and Racke (2008) found the solutions of the heat equation in the theory of TPL heat conduction in their recent research work. Also, Zenkour (2018) proposed a refined two-temperature multi-phase-lag (RPL) model for a generalized thermoelastic medium consisting of both the heat flux vector and the temperature gradient. In their work, Sardar et al. (2022) studied a three-dimensional coupled thermoelasticity for an anisotropic half-space using multi-phase lag gradients. Zenkour (2018) also studied the thermomechanical effects of microbeams using refined multiphase-lag theory. In association, Alharbi et al. (2022) studied a multi-phase-lag model to investigate the influence of variable thermal conductivity with initial stress on a fibre-reinforced thermoelastic material in the magnetic field.

In our recent study, we investigated the effect of multi-phase lag variables on a two-dimensional thermoelastic isotropic medium.

2 Formulation of the problem

In the orthogonal co-ordinate system XOY, we consider a two dimensional isotropic half-space defined in the region $W = \{0 \leq x < \infty, -\infty < y < \infty\}$ (as in Fig. 1) subject to traction free boundary $x = 0$. Also, y-axis is considered vertically downwards, and the xy-plane is along the free surface of the half-space.

3 Basic equations

Equation of motion:

For a homogeneous isotropic half-space, as in Ghosh et al. (2017), Zenkour (2018) and Eringen (1984), respectively, we consider the following governing equations.

$$(\lambda+\mu)\frac{\partial e}{\partial x}+\mu\nabla^2 u-\frac{P}{2}\frac{\partial^2 u}{\partial y^2}+\frac{P}{2}\frac{\partial^2 v}{\partial x\partial y}-\gamma\frac{\partial T}{\partial x}=\rho\left[\frac{\partial^2 u}{\partial t^2}-\Omega^2 u\right] \tag{1}$$

$$(\lambda+\mu)\frac{\partial e}{\partial y}+\mu\nabla^2 v+\frac{P}{2}\frac{\partial^2 u}{\partial x\partial y}-\frac{P}{2}\frac{\partial^2 v}{\partial x^2}+\gamma\frac{\partial T}{\partial y}=\rho\left[\frac{\partial^2 v}{\partial t^2}-\Omega^2 v\right] \tag{2}$$

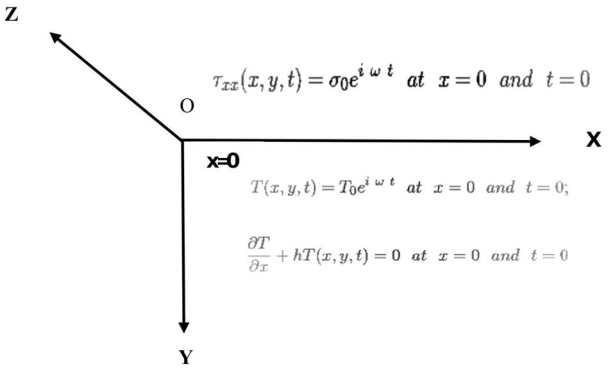

Fig. 1 Schematic diagram of the problem

The stress-displacement relation:

$$\tau_{xx} = (\lambda + 2\mu + P)\frac{\partial u}{\partial x} + (\lambda + P)\frac{\partial v}{\partial y} - \gamma T \tag{3}$$

$$\tau_{yy} = (\lambda + 2\mu + P)\frac{\partial v}{\partial y} + (\lambda + P)\frac{\partial u}{\partial x} - \gamma T \tag{4}$$

$$\tau_{xy} = \left(\mu - \frac{P}{2}\right)\frac{\partial v}{\partial x} + \left(\mu + \frac{P}{2}\right)\frac{\partial u}{\partial y} \tag{5}$$

Heat conduction equation *(In context of multi-phase Lag)***:**

$$\left(1 + \sum_{n=1}^{N} \frac{\tau_\theta^n}{n!}\frac{\partial^n}{\partial t^n}\right)\left(K_{11}\frac{\partial^2 T}{\partial x^2} + K_{22}\frac{\partial^2 T}{\partial y^2}\right)$$
$$= \left[\overline{R} + \tau_0\frac{\partial}{\partial t} + \sum_{n=1}^{N} \frac{\tau_q^{n+1}}{(n+1)!}\frac{\partial^{n+1}}{\partial t^{n+1}}\right]\left[\rho C_E\frac{\partial^2 T}{\partial t^2} + (3\lambda + 2\mu)\alpha_0 T_0\frac{\partial^2}{\partial t^2}\left(\frac{\partial u}{\partial x} + \frac{\partial v}{\partial y}\right)\right] \tag{6}$$

where $\gamma = (3\lambda + 2\mu)\alpha_t$, $\lambda + 2\mu = \rho {c_1}^2$ and $e = \frac{\partial u}{\partial x} + \frac{\partial v}{\partial y}$

4 Nomenclature

Column 1	Column 2
u, v: Displacement Components	e: Dilatation
T: Absolute thermodynamic temperature.	t: Time variable
C_E: Specific heat at constant strain	λ, μ: Lame's Constant
T_0: Reference temperature	τ: Relaxation Time
τ_q, τ_θ: Dual-phase-lag, τ_0: thermal relaxation time	ρ : Density of the material
K_{11}, K_{22} : Thermal conductivity	Ω: angular velocity in the domain W.
α_t : Coefficient of linear thermal expansion	P: Initial stress

5 Method of solution

5.1 Formulation of a vector-matrix differential equation

For the solution of equations (1)–(6), the physical quantities can be decomposed into the following form

$$\begin{array}{cc} t' = \frac{C_1^2}{K_1} t, \quad (x',\ y') = \frac{C_1}{K_1}(x, y), & (u', v') = \frac{c_1^3 \rho}{K_1(3\lambda+2\mu)\alpha_t T_0}(u, v), \\ \tau_0' = \frac{C_1^2}{K_1}\tau_0, & T' = \frac{T}{T_0} \\ (\tau_{xx}', \tau_{yy}', \tau_{xx}') = \frac{1}{(3\lambda+2\mu)\alpha_t T_0}(\tau_{xx}, \tau_{yy}, \tau_{xy}) & \Omega' = \frac{K_1}{C_1^2}\Omega,\ K_1 = \frac{K_{11}}{\rho C_E}, \\ \rho = \frac{\rho'}{\alpha T_0},\ c_1^2 = \frac{\lambda+2\mu}{\rho} & (\tau_q', \tau_\theta') = \frac{C_1^2}{K_1}(\tau_q, \tau_\theta) \end{array} \tag{7}$$

Introducing non-dimensional variables, we obtain from equations (1), (2) and (6) (omitting primes for convenience),

$$\frac{\partial^2 u}{\partial x^2} + C_{11}\frac{\partial^2 v}{\partial x \partial y} + C_{12}\frac{\partial^2 u}{\partial y^2} - \frac{\partial T}{\partial x} = \frac{\partial^2 u}{\partial t^2} - \Omega^2 u \tag{8}$$

$$\frac{\partial^2 v}{\partial y^2} + C_{21}\frac{\partial^2 v}{\partial x^2} + C_{22}\frac{\partial^2 u}{\partial x \partial y} + \frac{\partial T}{\partial y} = \frac{\partial^2 v}{\partial t^2} - \Omega^2 v \tag{9}$$

$$\begin{aligned} &\frac{K_{11}}{\rho C_E c_1^2}\left(1 + \sum_{n=1}^{N}\frac{\tau_\theta^n}{n!}\frac{\partial^n}{\partial t^n}\right)\left(\frac{\partial^2 T}{\partial x^2} + \frac{K_{22}}{K_{11}}\frac{\partial^2 T}{\partial y^2}\right) \\ &= \left(\overline{R} + \tau_0\frac{\partial}{\partial t} + \sum_{n=1}^{N}\frac{\tau_q^{n+1}}{(n+1)!}\frac{\partial^{n+1}}{\partial t^{n+1}}\right)\left(\frac{\partial^2 T}{\partial t^2} + \frac{\gamma^2 T_0}{\rho^2 c_1^2 c_E}\frac{\partial^2}{\partial t^2}\left(\frac{\partial u}{\partial x} + \frac{\partial v}{\partial y}\right)\right) \end{aligned} \tag{10}$$

After introducing non-dimensional variables, the stress-displacement relations (equations (3)–(5)) reduce to (omitting primes for convenience),

$$\tau_{xx} = C_{41}\frac{\partial u}{\partial x} + C_{42}\frac{\partial v}{\partial y} - T \tag{11}$$

$$\tau_{yy} = C_{41}\frac{\partial v}{\partial y} + C_{42}\frac{\partial u}{\partial x} - T \tag{12}$$

$$\tau_{yy} = C_{51}\frac{\partial v}{\partial x} + C_{52}\frac{\partial u}{\partial y} \tag{13}$$

5.2 Normal mode analysis

To decompose the physical variables in terms of normal modes, as in Ghosh et al. (2018), we consider the following normal mode analysis

$$(u, v, \tau_{xx}, \tau_{yy}, \tau_{xy}, T)(x, y, t) = (u^*, v^*, \tau_{xx}^*, \tau_{yy}^*, \tau_{xy}^*, T^*)(x)e^{\omega t + iay} \tag{14}$$

where ω is the angular frequency, a is the wave number along the x-axis, and $i = \sqrt{-1}$.

Introducing normal mode analysis to equation 8, 9 and 10, we obtain (omitting asterisks for convenience):

$$\frac{d^2u}{dx^2} = M_{11}u + M_{12}v + M_{13}T + M_{14}\frac{du}{dx} + M_{15}\frac{dv}{dx} + M_{16}\frac{dT}{dx} \tag{15}$$

$$\frac{d^2v}{dx^2} = M_{21}u + M_{22}v + M_{23}T + M_{24}\frac{du}{dx} + M_{25}\frac{dv}{dx} + M_{26}\frac{dT}{dx} \tag{16}$$

$$\frac{d^2T}{dx^2} = M_{31}u + M_{32}v + M_{33}T + M_{34}\frac{du}{dx} + M_{35}\frac{dv}{dx} + M_{36}\frac{dT}{dx} \tag{17}$$

Introducing normal mode analysis to equations (11)–(13), we obtain the stress components as (omitting asterisks for convenience)

$$\tau_{xx} = C_{41}\frac{du}{dx} + C_{42}\ \ iav - T \tag{18}$$

$$\tau_{yy} = C_{41}\ \ iav + C_{42}\frac{du}{dx} - T \tag{19}$$

$$\tau_{xy} = C_{51}\frac{dv}{dx} + C_{52}\quad iau \tag{20}$$

where M_{ij} $(i = 1, 2, 3$ and $j = 1, 2, .., 6)$ and C_{ij} $(i = 1, 2, 3, 4, 5$ and $j = 1, 2)$ are mentioned in the Appendix.

6 Solution of the vector-matrix differential equation

The equations (15)–(17) reduce to the compact form of vector-matrix differential equation as follows

$$\frac{d}{dx}(\vec{v}) = A\vec{v} \tag{21}$$

where $\vec{v} = \left(u \quad v \quad T \quad \frac{du}{dx} \quad \frac{dv}{dx} \quad \frac{dT}{dx}\right)$, and A is given in the appendix.

For the solution of the vector-matrix differential equation (21), we apply the method of eigenvalue approach as in Ghosh and Lahiri (2018). The characteristic equation of matrix A is given by

$$\left|A - \lambda I\right| = 0 \tag{22}$$

The roots of the characteristic equation (21) are $\lambda = \lambda_i$ $(i = 1(1)6)$, and the corresponding eigenvector $\mathbf{X}$ is given below

$$\mathbf{X} = [\delta_1 \quad \delta_2 \quad \delta_3 \quad \lambda\delta_1 \quad \lambda\delta_2 \quad \lambda\delta_3 \quad]^T \tag{23}$$

where

$$\begin{aligned} \delta_1 &= f_{11}f_{23} - f_{13}f_{22}, \\ \delta_2 &= f_{13}f_{21} - f_{11}f_{23}, \\ \delta_3 &= f_{11}f_{22} - f_{12}f_{21} \end{aligned} \tag{24}$$

and f_{ij} $(i, j = 1, 2, 3)$ are given in the Appendix.

The solution of the vector-matrix equation is given by

$$\begin{aligned} u &= \sum_{i=1}^{3} A_i(\delta_1)_{\lambda=-\lambda_i} e^{-\lambda_i x} \\ v &= \sum_{i=1}^{3} A_i(\delta_2)_{\lambda=-\lambda_i} e^{-\lambda_i x} \\ T &= \sum_{i=1}^{3} A_i(\delta_3)_{\lambda=-\lambda_i} e^{-\lambda_i x} \end{aligned} \tag{25}$$

Thus the stress components are as follows

$$\begin{aligned} \tau_{xx} &= \sum_{j=1}^{3} A_j R_{1j}(x), \\ \tau_{yy} &= \sum_{j=1}^{3} A_j R_{2j}(x), \\ \tau_{xy} &= \sum_{j=1}^{3} A_j R_{3j}(x), \end{aligned} \tag{26}$$

where R_{ij} $i, j = 1, 2, 3$ are given in the appendix, and A_j, $j = 1, 2, 3$ are to be obtained using the boundary conditions..

7 Boundary conditions

Due to the regularity condition of the solution at infinity, three terms containing exponentials of growing in nature in the space variables x have been discarded, and the remaining arbitrary constants A_i, $(i = 1, 2, \ldots 4)$ are to be determined from the following boundary conditions.

7.1 Mechanical boundary

The boundary of the half-space $x = 0$ has no traction elsewhere, i.e.,

$$\tau_{xx}(x, y, t) = \sigma_0 e^{i\omega t} \quad at \quad x = 0 \quad and \quad t = 0; \tag{27}$$

7.2 The thermal boundary condition

$$T(x, y, t) = T_0 e^{i\omega t} \quad at \quad x = 0 \quad and \quad t = 0; \tag{28}$$

$$\frac{\partial T}{\partial x} + hT(x, y, t) = 0 \quad at \quad x = 0 \quad and \quad t = 0; \tag{29}$$

Applying the above boundary conditions in equations (25) and (26), we get the following simultaneous equations:

$$\begin{aligned} A_1 S_{11} + A_2 S_{12} + A_3 S_{13} &= z_1 \\ A_1 S_{41} + A_2 S_{42} + A_3 S_{43} &= z_2 \\ A_1 S_{51} + A_2 S_{52} + A_3 S_{53} &= 0 \end{aligned} \tag{30}$$

The arbitrary constants can be obtained by solving the above simultaneous equations where, $A_i = \frac{D_i}{D}$, $i = 1, 2, 3$, D, D_i: $i = 1, 2, 3$, S_{ij}: $i, j = 1, 2, 3$ and z_i: $i = 1, 2$, which are given in the Appendix.

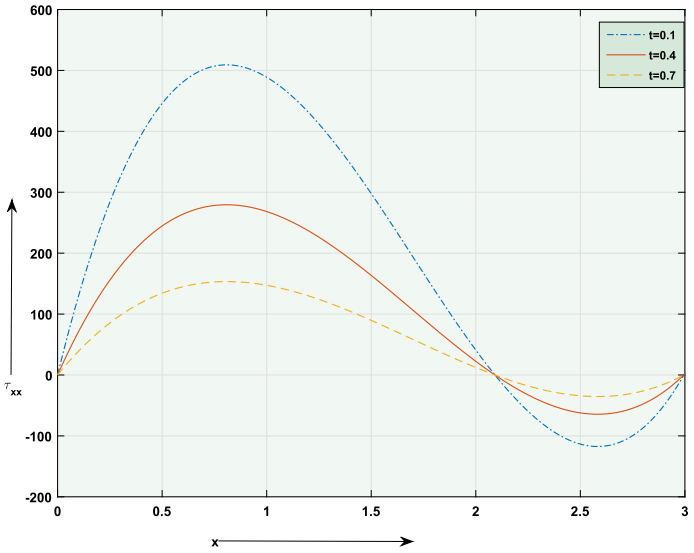

Fig. 2 Distribution of τ_{xx} vs. x for different t at y =0.7

8 Numerical analysis

Numerical analysis and computation have been done using the mechanical and thermal conditions mentioned in equations (27)–(29) to study the characteristic behaviors of the physical constants with respect to space variables in triclinic half-space. The numerical values (in SI units) of constants are taken as in Eringen (1984), Zenkour (2018):

$\lambda = 9.4 \times 10^{10}\ \mathrm{N/m^2}$, $\mu = 4.0 \times 10^{10}\ \mathrm{kg/ms^2}$, $\rho = 1.7 \times 10^3\ \mathrm{kg/m^3}$,
$a = 2.0,\ b = 0.5,\ T_0 = 293,$ $K, \alpha_T = 7.4033 \times 10^{-7}$ $K^{-1},\ t = 0.3s,\ \sigma_0 = 200.0,$
$K_{11} = 113 \times 10^{-4}\ \mathrm{N/m^2}$, $K_{22} = 117 \times 10^{-4}\ \mathrm{N/m^2}$, $C_E = 1.4 \times 10^3\ \mathrm{J/(kgk)}$,
$\gamma = 210 \times 10^4,\ \Omega = 0.5,$ $k = 348,\ \Omega = 0.5,$ $E_T = 0.0016,\ \omega = 2.0$

9 Geometrical representation and analysis

The expressions for displacements, stress, and temperature are very complex, and we prefer to develop an efficient computer program for numerical computations. We now depict some graphs to illustrate the problem.

10 Concluding remarks

Figure 2, 3 and 4 depict the characteristic behavior of the different stress components τ_{xx}, τ_{xy}, and τ_{yy}, respectively, along the x-axis with respect to the space variable (x) in different times (t=0.1, t=0.4, t=0.7). Also, Fig. 5, 6 and 7 represent the space variation of non-dimensional displacement components (u and v) and temperature (T) along the x-direction for different times mentioned in the legend.

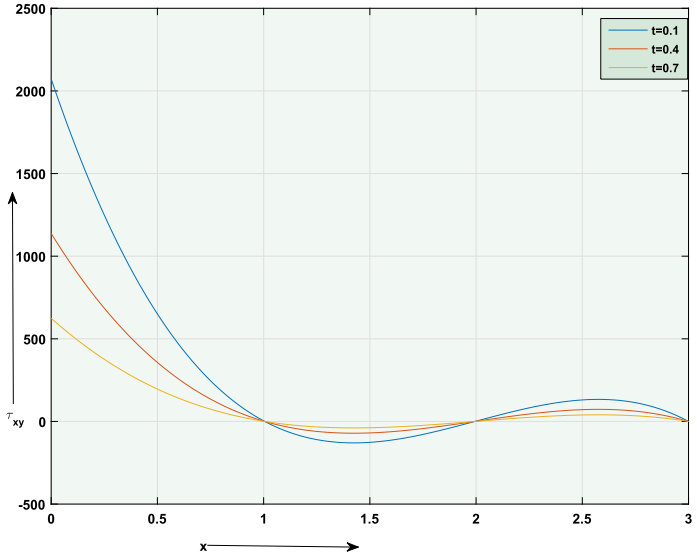

Fig. 3 Distribution of τ_{xy} vs. x for different t at y =0.7

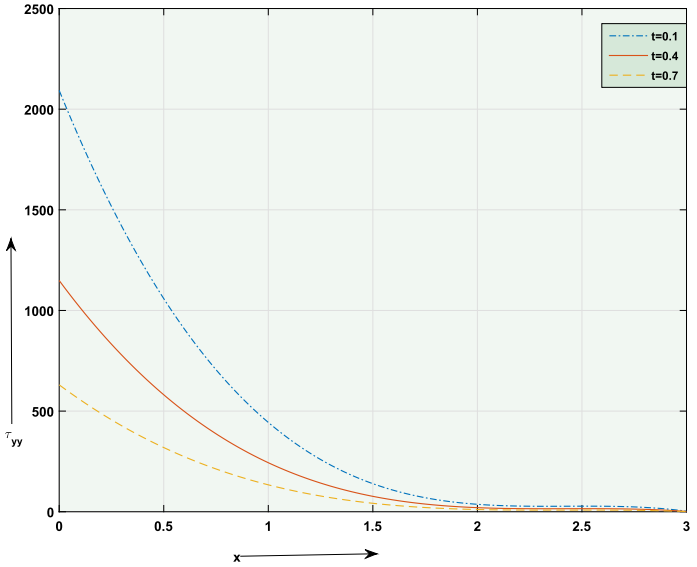

Fig. 4 Distribution of τ_{yy} vs. x for different t at y =0.7

Figure 8, 9, 10 and 11 are pointing out the three-dimensional variations of different stress components τ_{xx}, τ_{xy}, τ_{yy} and temperature (T), respectively, with respect to the space variable(x and y) in a particular time span (t=0.3).

Also, Fig. 12, 13 are about the three-dimensional depiction of the two elementary displacement components (u and v) w.r.t x and y for the fixed time (t=0.3).

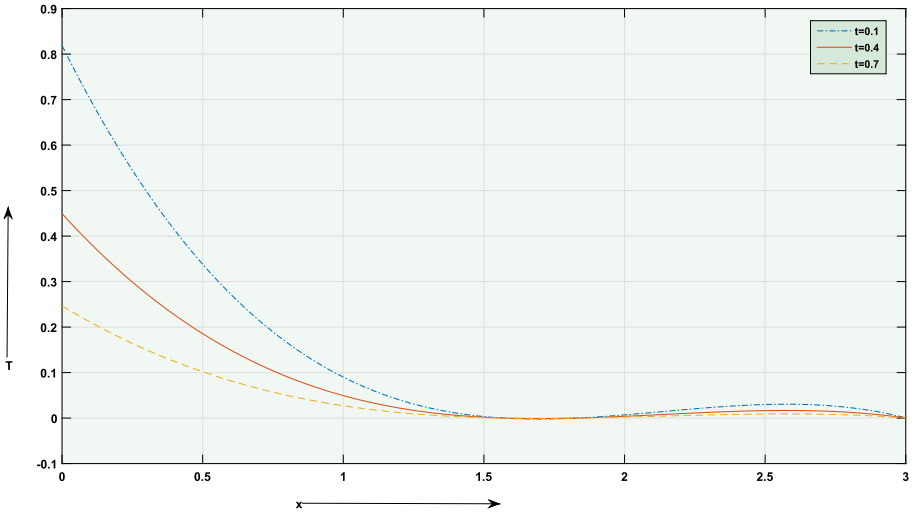

Fig. 5 Distribution of temperature (T) vs. x for different t at y =0.7

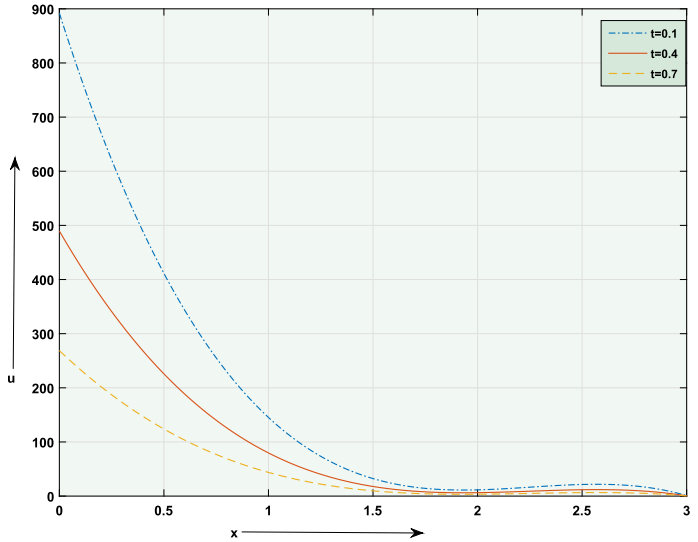

Fig. 6 Distribution of displacement component (u) vs. x for different t at y =0.7

11 Significance and applications

The Dual Phase Lag (DPL) model by Tzou, Chandrasekhariah and Three Phase Lag (TPL) by Roy Choudhury have been extended here using the refined technics known as the multi-phase lag model. In our work, the multi-phase lag concept is studied and verified successfully using the prominent mechanical and thermal boundary conditions associated with governing equations. The two- and three-dimensional variations of the different stress components, strain components and temperature curves have been represented graphically.

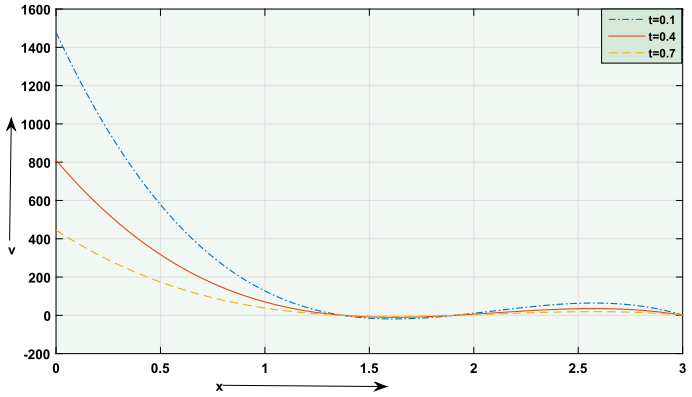

Fig. 7 Distribution of displacement component (v) vs. x for different t at y =0.7

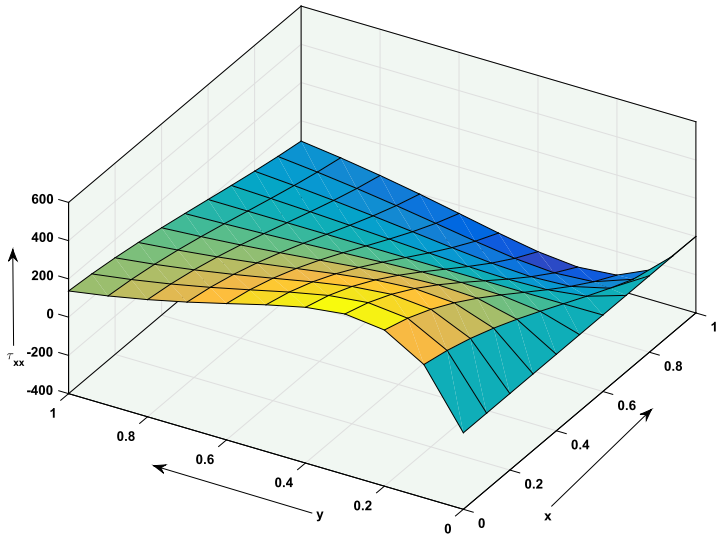

Fig. 8 Normal stress component, τ_{xx} as a function of x and y at time t=0.3

The tabular data in Fig. 14 represents the compact variations of the numerical value of different stress components, temperature and displacement components in the context of different thermoelastic models compared to the multi-phase lag model. From the data table, it is possible to differentiate the effect of different phase lag models and multi-phase lags on different physical variables.

Appendix 1

$$M_{11} = aC_{12} + \omega^2 - \Omega^2, \quad M_{12} = M_{13} = M_{14} = 0, \quad M_{15} = -iaC_{11}, \quad M_{16} = 1,$$

$$M_{21} = M_{25} = M_{26} = 0, \quad M_{22} = \frac{a^2 + \omega^2 + \Omega^2}{C_{21}}, \quad M_{23} = -\frac{ia}{C_{21}}, \quad M_{24} = -\frac{iaC_{22}}{C_{21}},$$

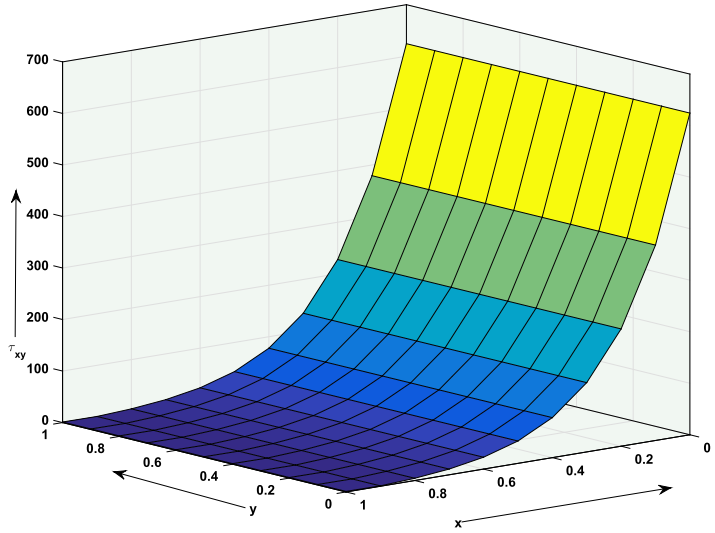

Fig. 9 Shearing tress, τ_{xy} as a function of x and y at time t=0.3

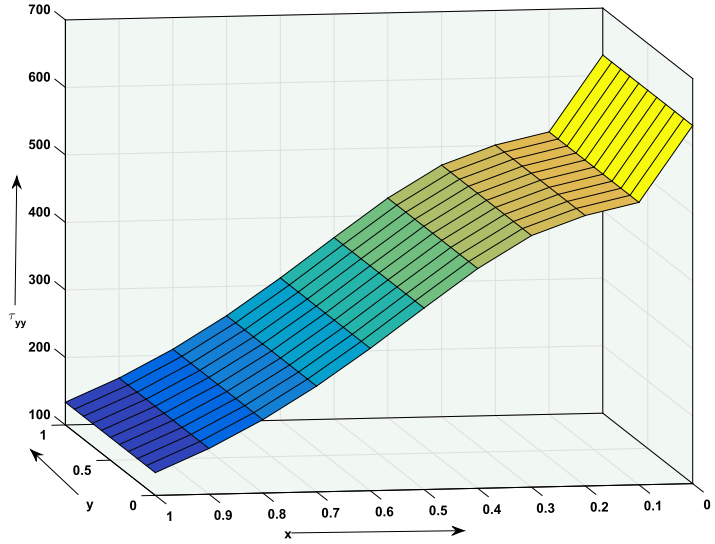

Fig. 10 Normal stress component, τ_{yy} as a function of x and y at time t=0.3

$$M_{31} = M_{35} = M_{36} = 0, \quad M_{32} = ia\frac{\gamma^2 T_0}{\rho^2 C_1^2 C_E},$$

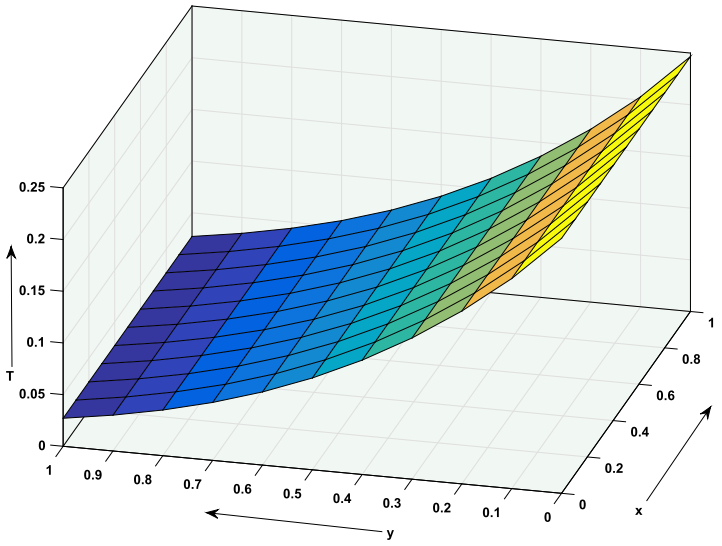

Fig. 11 Representation of temperature (T) as a function of x and y at time t=0.3

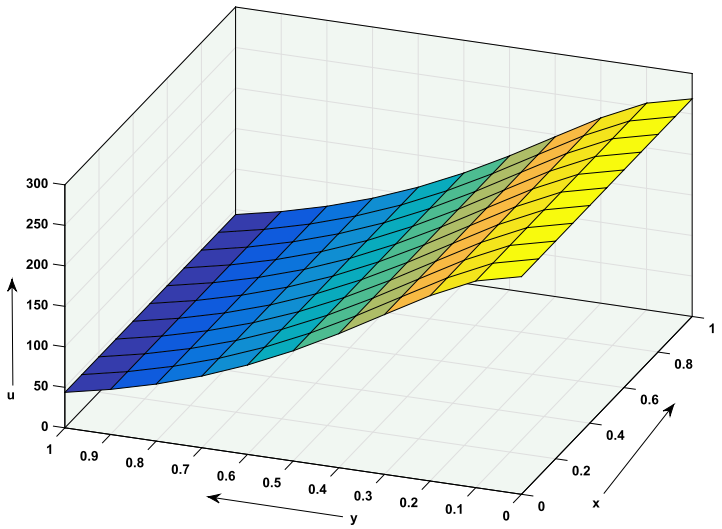

Fig. 12 Displacement field (u) as a function of x and y at time t=0.3

$$M_{33} = a^2 \frac{K_{22}}{K_{11}} + \frac{\omega^2 \left(\overline{R} + \tau_0 \omega + \sum_{n=1}^{N} \frac{\tau_q^{n+1}}{(n+1)!} \omega^{n+1} \right)}{\frac{K_{11}}{\rho C_E C_1^2} \left(1 + \sum_{n=1}^{N} \frac{\tau_\theta^n}{n!} \omega^n \right)},$$

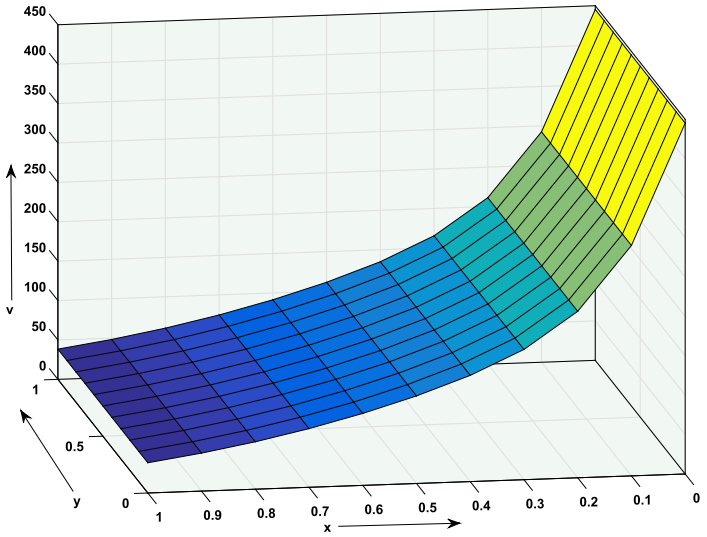

Fig. 13 Displacement field (v) as a function of x and y at time t=0.3

PHYSICAL VARIABLES	CTE	L-S	G-N -II	G-N -III	SPL	DPL	RPL				
							N=1	N=2	N=3	N=4	N=5
τ_{xx}	473.1505319	473.1502386	473.1494963	473.1505319	473.1505222	473.1502103	473.1502346	473.1502103	473.150038	473.1501995	473.1502717
τ_{yy}	472.6831795	472.6828864	472.6821447	472.6831795	472.6831697	472.6828581	472.6828824	472.68296	472.682686	472.6828473	472.6829194
τ_{xy}	134.462778	134.4626947	134.4624838	134.462778	134.4627753	134.4626866	134.4626936	134.4627156	134.4626377	134.4626836	134.4627041
u	197.2866122	197.28649	197.2861806	197.2866122	197.2866083	197.2864782	197.2864883	197.2865207	197.2864064	197.2864737	197.2865038
v	165.3005608	165.3004583	165.300199	165.3005608	165.3005573	165.3004484	165.3004569	165.300484	165.3003882	165.3004446	165.3004698
T	0.13659991	0.13659992	0.1365999	0.13659991	0.13659999	0.13659991	0.13659992	0.13659992	0.136599908	0.136599909	0.136599924

Fig. 14 Data table

$$M_{34} = \frac{\gamma^2 T_0}{\rho^2 C_1^2 C_E} \frac{\omega^2 \left(\overline{R} + \tau_0 \omega + \sum_{n=1}^{N} \frac{\tau_q^{n+1}}{(n+1)!} \omega^{n+1} \right)}{\frac{K_{11}}{\rho C_E C_1^2} \left(1 + \sum_{n=1}^{N} \frac{\tau_\theta^n}{n!} \omega^n \right)}$$

$$C_{11} = C_{22} = \frac{\lambda + \mu + \frac{P}{2}}{\lambda + 2\mu}, \quad C_{12} = C_{21} = \frac{\mu - \frac{P}{2}}{\lambda + 2\mu}$$

$$C_{41} = \frac{\lambda + 2\mu + \rho}{\rho c_1^2}, \quad C_{42} = \frac{\lambda + P}{\rho c_1^2}, \quad C_{51} = \frac{\mu - \frac{P}{2}}{\rho c_1^2}, \quad c_{52} = \frac{\mu + \frac{P}{2}}{\rho c_1^2}$$

$$A = \begin{pmatrix} L_{11} & L_{12} \\ L_{21} & L_{22} \end{pmatrix} \qquad L_{11} = \begin{pmatrix} 0 & 0 & 0 \\ 0 & 0 & 0 \\ 0 & 0 & 0 \end{pmatrix} \qquad L_{12} = \begin{pmatrix} 1 & 0 & 0 \\ 0 & 1 & 0 \\ 0 & 0 & 1 \end{pmatrix}$$

$$L_{21} = \begin{pmatrix} M_{11} & M_{12} & M_{13} \\ M_{21} & M_{22} & M_{23} \\ M_{31} & M_{32} & M_{33} \end{pmatrix} \qquad L_{22} = \begin{pmatrix} M_{14} & M_{15} & M_{16} \\ M_{24} & M_{25} & M_{26} \\ M_{34} & M_{35} & M_{36} \end{pmatrix}$$

$$\begin{array}{ccc} f_{11} = M_{11} + \lambda M_{14} - \lambda^2 & f_{21} = M_{21} + \lambda M_{24} & f_{31} = M_{31} + \lambda M_{34} \\ f_{12} = M_{12} + \lambda M_{15} & f_{22} = M_{22} + \lambda M_{25} - \lambda^2 & f_{32} = M_{32} + \lambda M_{35} \\ f_{13} = M_{13} + \lambda M_{16} & f_{23} = M_{23} + \lambda M_{26} & f_{33} = M_{33} + \lambda M_{36} - \lambda^2 \end{array}$$

$$R_{1i}(x) = [-C_{41}\lambda_i (delta_1)_{\lambda=\lambda_i} + iaC_{42}(\delta_2)_{\lambda=-\lambda_i} - (\delta_3)_{\lambda=\lambda_i}]e^{-\lambda_i x},\ i = 1, 2, 3$$

$$R_{2i}(x) = [iaC_{41}(\delta_2)_{\lambda=-\lambda_i} - C_{42}\lambda_1(\delta_1)_{\lambda=-\lambda_i} - (\delta_3)_{\lambda=-\lambda_i}]e^{-\lambda_i x},\ i = 1, 2, 3$$

$$R_{3i}(x) = [-C_{51}\lambda_i (\delta_2)_{\lambda=-\lambda_i} + iaC_{52}(\delta_1)_{\lambda=-\lambda_i}]e^{-\lambda_i x},\ i = 1, 2, 3$$

$$z_1 = \sigma_0 e^{i\omega t}$$

$$z_2 = T_0 e^{i\omega t}$$

$$S_{ij} = R_{ij}(0), \quad i = 1, 4, \quad j = 1, 2, 3$$

$$S_{5k} = R_{5k}(x), \quad k = 1, 2, 3$$

$$D_1 = \begin{vmatrix} z_1 & S_{12} & S_{13} \\ z_2 & S_{42} & S_{43} \\ 0 & S_{52} & S_{53} \end{vmatrix} \qquad D_2 = \begin{vmatrix} S_{11} & z_1 & S_{13} \\ S_{41} & z_2 & S_{43} \\ S_{51} & 0 & S_{53} \end{vmatrix}$$

$$D_3 = \begin{vmatrix} S_{11} & S_{12} & z_1 \\ S_{41} & S_{42} & z_2 \\ S_{51} & S_{52} & 0 \end{vmatrix} \qquad D = \begin{vmatrix} S_{11} & S_{12} & S_{13} \\ S_{41} & S_{42} & S_{43} \\ S_{51} & S_{52} & S_{53} \end{vmatrix}$$

Author contributions The authors contributed equally to this work.

Declarations

Competing interests The authors declare no competing interests.

References

Alharbi, A.M., Said, S.M., Abd-Elaziz, E.M., Othman, M.I.A.: Influence of initial stress and variable thermal conductivity on a fiber-reinforced magneto-thermoelastic solid with micro-temperatures by multi-phase-lags model. Int. J. Struct. Stab. Dyn. **22**(01), 2250007 (2022)

Chandrasekhariah, D.S.: Hyperbolic thermoelasticity: a review of recent literature. Appl. Mech. Rev. **21**(12), 705–729 (1998)

Eringen, A.C.: Plane waves in non local micropolar elasticity. Int. J. Eng. Sci. **22**(8–10), 1113–1121 (1984)

Ghosh, D., Lahiri, A.: Study on the generalized thermoelastic problem for an anisotropic medium. J. Heat Transf. **140**(9), 094501 (2018)

Ghosh, D., Lahiri, A.: Three Dimensional Fibre-Reinforce Anisotropic Half Space with Lagging Behavior in the Presence of Heat Source and Gravity. International Journal of Applied and Computational Mathematics **6**(40) (2020). Published online

Ghosh, D., Lahiri, A., Abbas, I.A.: Two-dimensional generalized thermo-elastic problem for anisotropic half-space. Math. Models Eng. **3**(1), 27–40 (2017)

Ghosh, D., Lahiri, A., Kumar, R., Roy, S.: 3D thermoelastic interactions in an anisotropic lastic slab due to prescribed surface temperature. J. Solid Mech. **10**(3), 502–521 (2018)

Ghosh, D., Das, A.K., Lahiri, A.: Modeling of a three dimensional thermoelastic half space with three phase lags using memory dependent derivative. Int. J. Appl. Comput. Math. **5**, 154–174 (2019)
Green, A.E., Lindsay, K.A.: Thermoelasticity. J. Elast. **2**(1), 1–7 (1972)
Green, A.E., Naghdi, P.M.: A re-examination of the basic postulates of thermomechanics. J. Math. Phys. Sci. **432**, 1885 (1991)
Green, A.E., Naghdi, P.M.: An undamped heat wave in an elastic solid. J. Therm. Stresses **15**, 253–264 (1992)
Green, A.E., Naghdi, P.M.: Thermoelasticity without energy dissipation. Elasticity **31**, 189–208 (1993)
Hetnarski, R.B., Ignaczak, J.: Soliton-like waves in a low temperature nonlinear thermoelastic solid. Int. J. Eng. Service **34**(15), 1767–1787 (1996)
Lord, H.W., Shulman, Y.: A generalized dynamical theory of thermoelasticity. J. Mech. Phys. Solids **15**(5), 299–309 (1967)
Quintanilla, R., Racke, R.: A note on stability in three-phase-lag heat conduction. Int. J. Heat Mass Transform. **51**, 24–29 (2008)
Roy Choudhuri, S.K.: On a thermoelastic three-phase-lag model. J. Therm. Stresses **30**(3), 231–238 (2007)
Sardar, S.S., Ghosh, D., Das, B., Lahiri, A.: On a multi-phase lag model of three-dimensional coupled thermoelasticity in an anisotropic half-space. In: Waves in Random and Complex Media (2022). Vol: Published online: 06 Jul 2022
Tzou, D.Y.: Unified field approach for heat conduction from micro- to macro-scales. SME J. Heat Transf. **117**, 8–16 (1995)
Tzou, D.Y.: Thermal shock phenomena under high rate response in solids. Heat Transf. Eng. **4**, 111–185 (1999)
Yang, F., Chong, A.C.M., Lam, D.C.C., Tong, P.: Couple stress based strain gradient theory for elasticity. Int. J. Solids Struct. **39**, 2731–2743 (2002)
Zenkour, Ashraf M.: Refined microtemperatures multi-phase-lags theory for plane wave propagation in thermoelastic medium. Results Phys. **11**, 929–937 (2018)
Zenkour, Ashraf M.: Refined two-temperature multi-phase-lags theory for thermomechanical response of microbeams using the modified couple stress analysis. Acta Mech. **229**, 3671–3692 (2018)